AAPS PharmSciTech (2024) 25:95
https://doi.org/10.1208/s12249-024-02814-w

RESEARCH ARTICLE

Verapamil-Loaded Cubosomes for Enhancing Intranasal Drug Delivery: Development, Characterization, *Ex Vivo* Permeation, and Brain Biodistribution Studies

Mennatullah M. Faisal[1] · Eman Gomaa[1] · Adel Ehab Ibrahim[2] · Sami El Deeb[3] · Ahmed Al-Harrasi[2] · Tarek M. Ibrahim[1]

Received: 29 January 2024 / Accepted: 20 April 2024

Abstract

Verapamil hydrochloride (VRP), an antihypertensive calcium channel blocker drug has limited bioavailability and short half-life when taken orally. The present study was aimed at developing cubosomes containing VRP for enhancing its bioavailability and targeting to brain for cluster headache (CH) treatment as an off-label use. Factorial design was conducted to analyze the impact of different components on entrapment efficiency (EE%), particle size (PS), zeta potential (ZP), and percent drug release. Various *in-vitro* characterizations were performed followed by pharmacokinetic and brain targeting studies. The results revealed the significant impact of glyceryl monooleate (GMO) on increasing EE%, PS, and ZP of cubosomes with a negative influence on VRP release. The remarkable effect of Poloxamer 407 (P407) on decreasing EE%, PS, and ZP of cubosomes was observed besides its influence on accelerating VRP release%. The DSC thermograms indicated the successful entrapment of the amorphous state of VRP inside the cubosomes. The design suggested an optimized formulation containing GMO (50% w/w) and P407 (5.5% w/w). Such formulation showed a significant increase in drug permeation through nasal mucosa with high E_r value (2.26) when compared to VRP solution. Also, the histopathological study revealed the safety of the utilized components used in the cubosomes preparation. There was a significant enhancement in the VRP bioavailability when loaded in cubosomes owing to its sustained release favored by its direct transport to brain. The I.N optimized formulation had greater BTE% and DTP% at 183.53% and 90.19%, respectively in comparison of 41.80% and 59% for the I.N VRP solution.

Keywords brain targeting efficiency · cubosomes · *ex vivo* permeation · factorial design · pharmacokinetic study

Introduction

Verapamil hydrochloride (VRP) is classified as calcium channel blocker prescribed for hypertension, cardiac arrhythmia, angina, etc. [1]. It is also reported as a concomitant therapy for the management of cluster headache (CH) as an off-label use [2, 3]. As reported, it significantly reduced cluster attack frequency and decreased the requirement for ineffective treatments [4]. CH is an extremely severe unilateral headache which strikes many times a day and is associated with ipsilateral autonomic symptoms. Its daily attacks may continue for hours and present as a series (cluster cycle) that may remain for months. This cycle may be followed by a remission period with no apparent symptoms for months or years [5]. Therefore, VRP is prescribed as a first-line prophylactic treatment to decrease the CH

✉ Adel Ehab Ibrahim
adel@unizwa.edu.om

✉ Sami El Deeb
s.eldeeb@tu-bs.de

1 Department of Pharmaceutics, Faculty of Pharmacy, Zagazig University, Zagazig 44519, Egypt

2 Natural and Medical Sciences Research Center, University of Nizwa, Birkat Al Mauz, P.O. Box 33, Nizwa 616, Sultanate of Oman

3 Institute of Medicinal and Pharmaceutical Chemistry, Technische Universität Braunschweig, 38106 Brunswick, Germany

Published online: 06 May 2024

severity and reduce the episodes' frequency during the cluster period [2, 6, 7].

VRP is reported to have poor oral bioavailability (20–35%) related to its hepatic first pass metabolism [8]. Regarding the high solubility and short half-life of VRP, it is a good opportunity to formulate VRP in sustained release preparations for enhancing its bioavailability and extending its pharmacological effect [9].

The intranasal (I.N) route has been elicited as a safe pathway for the effective and rapid management of the CH attacks which are frequently accompanied with severe nausea or vomiting, since the oral administration of drugs may be accompanied by poor gastrointestinal absorption [10]. Consequently, the I.N route, by transporting the drugs along the olfactory sensory neurons, can offer an appealing alternative to oral route [11]. Being non-invasive and painless with no requirements of sterility regulations and physician interventions makes the I.N route promising for drug delivery, especially when targeting the central nervous system. The limitations concerned with the rapid mucociliary clearance can be solved by using mucoadhesive delivery systems for prolonging the contact time with the nasal mucosa [12]. Several nano-colloidal systems proved their efficiency to deliver drugs from the nose directly to the brain, for examples, liposomes [13], niosomes [14], polymeric micelles [15], cubosomes [16], etc. They can physically shield drugs from degradation resulting in boosting their penetration through the nasal mucosa and prolonging their residence at the absorption site [17].

Cubosomes are exceptional nano-colloidal delivery systems whose attractive assembly with a considerable size (10–500 nm) allows them to highly encapsulate many hydrophilic, lipophilic, or amphiphilic drugs [18]. Moreover, biocompatibility, low toxicity, thermodynamic stability, and bioadhesiveness of cubosomes with controlled release properties promote the nasal drug delivery [16]. Glyceryl monooleate (GMO) is an amphiphilic non-toxic and non-irritant polar lipid which can be self-assembled as a honeycomb-like network forming three-dimensional (3D) cubic nano-structures capable for encapsulating the drug candidates [19, 20]. In addition, the presence of non-ionic block copolymers, such as Poloxamer 407 (P407) can enhance the cubosomal stability by preserving the bi-continuous internal structure of cubosomes [21]. Corresponding to the bioadhesion features of cubosomes and their structure resembling the human biomembranes [22], they were selected in our study to examine their capability to encapsulate VRP and the possibility of drug targeting to the brain via the I.N route.

The organized Design of experiments (DoE) system is used to study the relation between various factors and their influence on the experimental outputs [23]. One of its distinctive tools is the factorial design which is more preferred for prediction of responses owing to its flexibility concerning the studied factors and the experimental runs [24]. The optimization technique can be offered leading to producing an innovative product having eligible characteristics [25, 26]. Therefore, three-levels factorial design was followed in this study to differentiate between the factors that can influence the studied responses and the appropriate level of each factor that can exhibit a better optimized output.

Our study aimed at developing nano-structured cubosomes containing VRP using factorial design to study the impact of changing the components' concentrations on the properties of cubosomes. Various *in-vitro* characterizations of optimized formulation were conducted. In comparison to the pure VRP solution, the *ex-vivo* drug permeation through nasal sheep mucosa was studied for the optimized formulation to examine the VRP diffusion through the nasal membrane. Additionally, the optimized formulation was evaluated for its safety, efficacy, and suitability for the I.N administration with assessment of the VRP bioavailability in the rat plasma and its biodistribution into brain.

Materials and Methods

Materials

VRP was kindly supplied by Arabian Drug Co., Cairo, Egypt. GMO was gifted by Gattefossé, Saint-Priest, France. P407 was purchased from Sigma Chemical Co., St. Louis, MO, USA. Other solvents and chemicals were of high analytical grade.

Experimental Design

A factorial design of two-factors and three-levels (3^2) was set aiming to statistically analyze different factors for nine cubosomal formulations (Design Expert®, Stat-Ease Inc, Minneapolis, MN, USA). The levels were fitted as low, medium, and high. The independent factors were GMO concentration (factor A; 25–50% w/w) and P407 concentration (factor B; 2.5–10% w/w). The dependent responses were entrapment efficiency (EE%) (Y_1), particle size (PS) (Y_2), zeta potential (ZP) (Y_3), and drug release percent after 5 h (Y_4). The analysis of variance (ANOVA) at a probability level ($p < 0.05$) was used to analyze the experimental results and determine the significance of studied terms. The one factor and interaction plots were studied to observe the relationship between the factors and responses.

Preparation of VRP-loaded Cubosomes

Different VRP-loaded cubosomes were prepared by the melt dispersion emulsification method [20]. The concentrations of GMO and P407 given by the design software were followed. In a glass vial, GMO as the lipid phase was melted together with P407 as a surfactant in a hot water bath at 70°C. The melted preparations were injected dropwise into an aqueous solution (4 g) containing 50 mg VRP at 70°C with continuous vortexing at high speed (3,300 rpm) till obtaining homogenous dispersions. After equilibration for 48 h at ambient temperature, they were dispersed with distilled water by vortexing to get a final weight of 10 g containing 5 mg/g of VRP (0.5% w/w). Afterwards, some formulations showed gel appearance and were termed as cubosomal gels (cubo-gels), while others remained as cubosomal dispersions. The formulations were stored overnight at the ambient temperature for further studies.

In-vitro Characterization and Optimization of Cubosomes

EE% Measurement

The VRP amounts successfully entrapped in cubosomes were indirectly measured. The non-entrapped VRP was separated by diluting each cubosomal formulation (1 mL) with 1 mL distilled water followed by centrifugation for 2 h at 4°C and 21,380 × g [27]. The free drug in the supernatant was estimated spectrophotometrically at 275 nm. The EE% was calculated by this equation:

$$EE\% = \frac{\text{Total drug content} - \text{Free drug content}}{\text{Total drug content}} \times 100$$

PS, polydispersity Index (PDI), and ZP Measurement

The PS and PDI parameters were determined by a Zetasizer instrument (Nano–ZS90, Malvern Instruments Ltd., Malvern, UK) using dynamic light scattering (DLS) technique. The formulations were diluted in a ratio of 1:10 in distilled water (refractive index = 1.33), carefully mixed to prevent multi-scattering, and then placed in disposable sizing cuvettes. To measure ZP, the diluted samples were placed in a clear disposable zeta cuvettes and the measurements were conducted at 25°C [28].

In-vitro VRP Release Study

The study was performed using dialysis membranes (cut-off 12,000–14,000 Da) loaded with cubosomes equivalent to 5 mg of VRP. The bags were immersed in 15 mL of phosphate buffer saline (PBS) of pH 7.4 [29], as a receiver medium, in a shaking water bath at 37°C and 50 rpm. At different time intervals, aliquots were withdrawn and replaced with fresh buffer solutions. The released VRP amounts were determined spectrophotometrically at 275 nm in comparison to pure VRP solution in order to highlight the effect of using cubosomes on the drug release [30].

Optimized Formulation Selection

The software optimized a suitable formulation according to the required goal criteria (maximized Y_1 and Y_3 and minimized Y_2 and Y_4). The relation between the experimental Y_1-Y_4 values of optimized formulation and those predicted by the design was studied.

In-vitro Characterization of Optimized Cubo-Gel

Transmission Electron Microscopy (TEM)

The morphology of optimized formulation was performed using a transmission electron microscope. The sample was diluted and placed on a 200-mesh carbon-coated copper grid and the excess fluid was removed using a filter paper. It was stained with 1% sodium phosphotungstate solution and examined under the microscope operating at 80 kV [31].

Drug Release Kinetics

The drug release data of the optimized formulation were analyzed according to zero order, first order, Higuchi, Hixson-Crowell, and Korsmeyer-Peppas models to describe the pattern of drug release based on the correlation coefficient (R^2) values.

Stability Study

To monitor the optimized formulation during storage, it was stored at 4°C and 25°C for 3 months. The four responses were compared with those of fresh formulation by Student's t test using GraphPad Prism® software.

Differential Scanning Calorimetry (DSC)

To detect any changes in the VRP physical state when entrapped within the optimized formulation, the DSC study was performed on VRP powder, GMO, P407, plain formulation (cubosome with no added drug), and VRP-loaded optimized formulation. Samples were heated at 10°C/min in an aluminum pan under a nitrogen atmosphere using a DSC instrument.

Physical Evaluation

The pH of optimized formulation was measured to ensure its safety and absence of any possible irritation after I.N application. The formulation (1 g) was diluted by 10 mL distilled water and the pH was measured using a pH meter. The gel strength of optimized formulation was measured. The time required for a specific weight (3.5 g) to penetrate the gel sample (5 g) for 3 cm was recorded. The time would be acceptable within 25–50 s [32]. The mucoadhesive strength was also determined using a modified physical balance. The force required to detach the formulation from a nasal membrane was recorded. As described by Abdulla *et al.* [11], the left part of balance consisted of two vials attached from their bases. Each base was attached with a nasal mucosa. The optimized formulation was placed on the lower base and then the glass vials were held together. The right part of balance was replaced with an empty cup filled slowly with water at a constant rate until the vials were detached. The mucoadhesive strength (dyne/cm^2) was calculated by this equation:

$$\text{Mucoadhesive strength} = \frac{m \times g}{A}$$

where, m was the added water weight in grams, g was the gravity acceleration (980 cm/s^2), and A was the mucosa area (cm^2).

Ex-vivo Permeation Study

The permeation of VRP through nasal mucosa compared to the VRP solution was conducted through separation of nasal mucosa from its connective tissue and was immersed in PBS (pH 7.4) containing 0.02% sodium azide as a preservative overnight for equilibration [11]. Nasal membranes of suitable sizes were fixed to locally fabricated diffusion cells with 15 cm length and internal diameter of 2.9 cm and filled with the optimized formulation or VRP solution, both equivalent to 5 mg drug. The receptor compartment was 15 mL PBS (pH 7.4) that was transferred to a shaking water bath stirred at 50 rpm and 37°C ± 0.5°C. At various time intervals, 2 ml aliquots were removed for 24 h and the amounts of drug permeated were determined spectrophotometrically at 275 nm. A plot was made from the average cumulative amount of drug permeated per unit surface area of the nasal mucosa *versus* time, then the steady state flux (J_{ss}) values were estimated from slope of the linear portion of the plots. The J_{ss} values were divided by the total amount of drug to get the permeability coefficient (K_p). The enhancement ratio (E_r) was calculated by dividing the formulation K_p by the control K_p [33]. The results were analyzed using Student's t test by GraphPad Prism® software.

Histopathological Evaluation

The mucosal sample was taken after completion of the *ex-vivo* study after 24 h to examine the biocompatibility of the optimized formulation with the nasal tissues. For comparison, a normal mucosal piece treated with normal saline (negative control), an excised piece immersed in PBS (pH 7.4) containing 0.02% sodium azide overnight for equilibration, and other mucosal piece treated with isopropyl alcohol (positive control), were used. The mucosal samples were washed with saline after 1 h and retained in formalin overnight. They were cut and dehydrated using an ethanol gradient. They were solidified in paraffin blocks and small sections were cut and examined microscopically (× 100) after applying hematoxylin and eosin stain [11, 12].

In-vivo Characterization of Optimized Cubo-Gel

Ethical approval

The animal experiments were performed according to the guidelines of Institutional Animal Care and Use Committee (IACUC) of Faculty of Pharmacy, Zagazig University, Egypt (ZU-IACUC/3/F/49/2022).

***In-vivo* Biodistribution Analysis** Three groups of adult albino rats (200–250 g) were used (n = 6). Group A received 1 mL of VRP intravenous (I.V) solution containing a drug dose calculated as 10 mg of drug per Kg of rat weight [34]. By using a micropipette, Group B received I.N optimized VRP-loaded formulation (10 mg/Kg) and group C received I.N VRP solution (10 mg/Kg). The rats were firmly held from their back during the I.N administration after sedating by diethyl ether inhalation to avoid sneezing during the I.N instillation [16, 35]. The three groups were divided into seven time-based subgroups and sacrificed at different time intervals (10, 15, 30, 60, 120, 240, and 480 min). The blood was collected using a cardiac puncture and stored in heparinized tubes for further studies. Blood samples were centrifuged at 4,180 × g for 10 min and the plasma was separated and kept in -20°C for further analysis using high performance liquid chromatography (HPLC) using a reversed phase RP-C18 column (Kinetix® 5 µm, 150 × 4.6 mm) from Phenomenex (CA, USA).

The brain tissues were separated, rinsed with 0.9% NaCl, and cleared from the adhering tissues [36]. They were homogenized with normal saline (4 mL for 1 g tissue) and the homogenates were centrifuged at 4,180 × g for 15 min at 4°C. The supernatants were stored at -20°C until the drug analysis by HPLC.

Samples Preparation and Parameters Calculation The method described by Mouez *et al.* [37] was followed with little modi-

fications for quantifying VRP using HPLC. Exactly, 1 mL of brain homogenate and 0.5 mL of plasma samples were individually mixed with nicardipine HCl as an internal standard. Each sample was mixed with 1 mL acetonitrile, vortexed for 2 min, and centrifuged at 10,413×g for 15 min. The supernatants were filtered through membrane filters (0.45 µm) and injected into the HPLC system for analysis. The mobile phase consisted of acetonitrile:methanol:0.01 M disodium hydrogen phosphate (55%:15%:30%) and was adjusted to pH 5.2 with 50% phosphoric acid. The flow rate was set at 1 mL/min and the detection wavelength was 235 nm.

Different pharmacokinetic parameters namely maximum plasma concentration (C_{max}), time required to reach the C_{max} (T_{max}), area under the curve ($AUC_{0\text{-}24\ h}$), area under the curve from time zero to infinity ($AUC_{0\text{-}\infty}$), and half-life ($t_{1/2}$) were calculated. The brain targeting efficiency (BTE%) and the drug transport percentage (DTP%) were calculated [36]. The BTE% was the ratio of the drug level in the brain acquired with the I.N administration *versus* the I.V administration. The BTE% was calculated by this equation:

$$BTE\% = [(Brain_{I.N}/Plasma_{I.N})/(Brain_{I.V}/Plasma_{I.V})] \times 100$$

The $Brain_{I.N}$ is the $AUC_{0\text{-}\infty}$ in the brain homogenate and $Plasma_{I.N}$ is the $AUC_{0\text{-}\infty}$ in the plasma after the I.N application of optimized formulation and drug solution. The $Brain_{I.V}$ and $Plasma_{I.V}$ are the $AUC_{0\text{-}\infty}$ in the brain homogenate and plasma after the I.V administration, respectively. The values of BTE% above 100% indicated an efficient brain targeting after I.N administration.

The DTP% is the proportion of the I.N dose that is transported directly from the nose to the brain compared to the total quantity of drug reaching the brain following the I.N administration. It was calculated by these equations:

$$DTP\% = \left(\frac{Brain_{I.N} - Brain_{x}}{Brain_{I.N}}\right) \times 100$$

$$Brain_{x} = \left(\frac{Brain_{I.V}}{Plasma_{I.V}}\right) \times Plasma_{I.N}$$

where, $Brain_x$ is the brain AUC fraction participated by the systemic circulation through the blood brain barrier (BBB) after the I.N administration.

The differences between the groups were tested using one way ANOVA by GraphPad Prism® software.

Results

Preparation of VRP-Loaded Cubosomes

The cubosomes loaded with VRP were prepared through disrupting GMO and P407 as a stabilizer by using a mechanical stirrer. After equilibration and dilution with distilled water, 5 mg/mL of VRP was maintained constant for the prepared formulations. The cubosomes showed uniform opaque mixtures with white colors and no aggregation signs. Some formulations having high GMO concentrations demonstrated gel appearance, such as F1, F3, F5, F7, and F9, whereas the others appeared as cubosomal dispersions. The cubosomes were prepared at a temperature above the GMO melting point resulting in emulsification of GMO with water without using gelling agents [38].

Experimental Design and Optimization

The ANOVA results showed the significance of models due to their high F-values (71.33, 76.84, 61.91, and 66.46 for the Y_1, Y_2, Y_3, and Y_4 models, respectively) having p values < 0.05 indicating the low chance of the error present. The terms having p values < 0.05 were considered significant (Table I).

Besides, the R^2 could measure the variation around the mean explained by the model. The closeness of the R^2 values to 1 could indicate the good relationship between the experimental and predicted values for each model [39]. The low difference between adjusted and predicted R^2 values (less than 0.2) would be acceptable by the design. Moreover, the higher adequate precision values (greater than 4) could indicate an adequate signal/noise ratio (Table I).

The polynomial equations for the models were also determined (Table I). The synergistic effects could be indicated from the positive signs of the coefficients, while the antagonistic effects could be indicated from those of negative signs [40].

EE% Analysis

The EE% values of cubosomes ranged from 24.13% to 80.18% indicating that various EE% values could be obtained by different changes in the concentrations of cubosomes' components (Table II). The EE% increased significantly by increasing the amount of incorporated lipid (Fig. 1a). While, increasing P407 concentration showed a significant decrease in the VRP entrapment in the cubosomal formulations (Fig. 1b).

The 3D response surface graphs were plotted for studying the interactions of independent factors by observing the effect of changing the levels of them on the response. Parallelism of each two opposite lines could indicate the absence of interaction between the factors. The interaction between the two studied independent factors was absent (Fig. 1c). Additionally, the quadratic term of factor A showed a significant negative impact on the Y_1 response as supported by its low p value (0.0075) and its negative sign in the polynomial equation (Table I).

Table I Statistical Analysis of Four Responses by ANOVA

Source	Y_1 response *p* values	Y_2 response	Y_3 response	Y_4 response
A	0.0005*	0.0018*	0.0009*	0.0005*
B	0.0156*	0.0006*	0.0001*	0.0054*
AB	0.1724	0.0119*	0.0114*	0.0444*
A^2	0.0075*	0.3218	0.6240	0.1399
B^2	0.4910	0.4365	0.4027	0.9533
	Fit statistics			
R^2	0.9917	0.9923	0.9964	0.9911
Adjusted R^2	0.9778	0.9793	0.9905	0.9761
Predicted R^2	0.9038	0.9288	0.9582	0.8909
Adequate precision	21.8865	26.0649	38.3441	23.5186
	Coded equations			
Y =	66.86 + 23.34 A – 6.86 B – 3.02 AB – 15.49 A^2 – 1.87 B^2	160.50 + 29.65 A – 43.45 B – 18.88 AB – 5.75 A^2 + 4.35 B^2	28.39 + 1.80 A – 3.90 B – 1.27 AB – 0.3067 A^2 + 0.0833 B^2	84.35 – 17.96 A + 8.01 B + 4.51 AB – 3.82 A^2 – 0.1217 B^2

A, GMO concentration; B, P407 concentration; Y_1, entrapment efficiency (EE%); Y_2, particle size (PS), Y_3, zeta potential (ZP); Y_4, drug release percent after 5 h; R^2, multiple correlation coefficient; *, significant

Table II Composition of Prepared Cubosomes and Observed Values of Tested Parameters

Formula	A (% w/w)	B (% w/w)	Y_1 response (%)	Y_2 response (nm)	Y_3 response (mV)	Y_4 response (%)
F1	50	2.5	80.18 ± 2.1	253.20 ± 18.2	-35.12 ± 1.3	51.79 ± 1.1
F2	25	6.25	27.02 ± 0.9	125.40 ± 14.2	-26.06 ± 1.8	99.96 ± 2.3
F3	37.5	10	56.25 ± 1.9	115.90 ± 10.2	-25.16 ± 1.2	94.52 ± 0.5
F4	25	10	24.13 ± 0.8	105.90 ± 12.9	-23.63 ± 1.1	99.99 ± 2.1
F5	50	6.25	77.18 ± 2.1	177.80 ± 16.5	-30.36 ± 0.9	61.12 ± 0.9
F6	25	2.5	29.21 ± 1.1	152.70 ± 19.5	-29.35 ± 0.8	95.28 ± 1.2
F7	37.5	6.25	65.41 ± 1.7	166.80 ± 11.9	-28.15 ± 0.8	84.33 ± 1.7
F8	50	10	63.04 ± 1.9	130.90 ± 12.8	-25.34 ± 0.9	74.56 ± 1.1
F9	37.5	2.5	75.19 ± 2.1	207.50 ± 14.1	-32.04 ± 1.1	73.95 ± 0.8

A, GMO concentration; B, P407 concentration; Y_1, entrapment efficiency (EE%); Y_2, particle size (PS), Y_3, zeta potential (ZP); Y_4, drug release percent after 5 h

PS Analysis

The PS values of cubosomes were in the range of 105.9 nm to 253.20 nm (Table II). Increasing the GMO concentration increased the PS of cubosomes in a significant manner (Fig. 1d). On the other hand, increasing the P407 concentrations was accompanied by a significant decrease in the particle size (Fig. 1e). Concerning studying the interaction effects (AB factor), a clear interaction effect was observed between the A and B factors on the Y_2 response as represented by the non-parallelism of each two opposite lines (Fig. 1f).

Furthermore, the PDI values of cubosomes were measured. The values were ranged from 0.31 to 0.47 (Table S1 supplementary material) which were lower than 0.5 recommending the homogeneous distribution of the cubosomal formulations [41].

ZP Analysis

The ZP is an indicator revealing the physical stability of cubosomes. The ZP values ranged between -23.63 mV and -35.12 mV (Table II). Increasing the GMO concentration showed a remarkable increase in the absolute ZP values (Fig. 2a). While P407 showed a significant negative effect on the ZP values (Fig. 2b). Furthermore, a significant interaction effect between the two factors on the Y_3 response was observed where each two opposite lines were non-parallel to each other (Fig. 2c).

In-vitro VRP Release Analysis

Figure 3 illustrates the release pattern of VRP from different cubosomal formulations. The F1 showed the highest

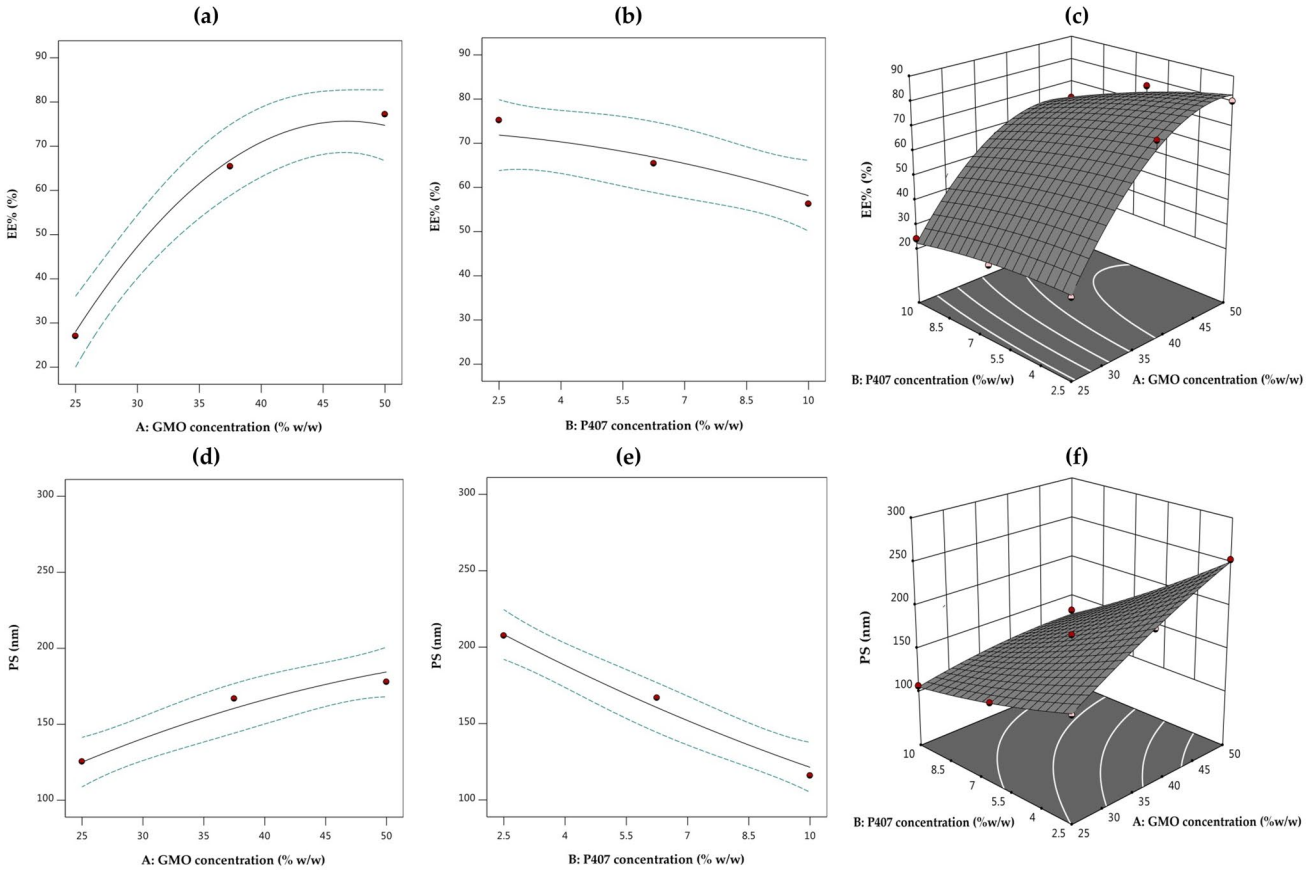

Fig. 1 One factor and 3D response surface graph showing the effect of **a** A on Y_1 **b** B on Y_1 **c** AB on Y_1 **d** A on Y_2 **e** B on Y_2 **f** AB on Y_2

sustained release with 65.96% at the end of 24 h. This could be attributed to the higher EE% of F1 formulation. The release was faster when the EE% decreased in the cubosomes. Some formulations with lower EE% showed less sustained release till 5 h only, such as F4 and F2 having EE% values of 24.13% and 27.02%, respectively. Others showed more sustained release for 6 h, such as F3 and F6 having EE% values of 56.25% and 29.21%, respectively. The more sustained release was observed in F1, F5, F7, F8, and F9 formulations and this might be related to the higher EE% of these formulations (80.18%, 77.18%, 65.41%, 63.04%, and 75.19%, respectively).

Figure 2d-e display that VRP could show a significant changeable release profile corresponding to the alterations in the GMO and P407 concentrations. The effect of the AB interactive factor on the Y_4 response was also significant (Fig. 2f) where each of the two opposite lines showed a non-parallelism.

Optimized Formulation Selection

Corresponding to the required goals, the software suggested an optimized formulation comprising of GMO (50% w/w) and P407 (5.5% w/w) with a visual gel appearance. The predicted values by the design were 76.61%, 197.02 nm, -31.07 mV, and 60.06% for the four responses, respectively. In comparison, the experimental values of responses were 77.24%, 210.49 nm, -30.34 mV, and 61.91%, respectively. The feasible consistence between the experimental and predicted values could reflect the validity of the models.

The optimized formulation showed a slight initial burst release followed by a sustained release over the time of the experiment (Fig. 4a). It showed about 69.87% of drug released after 24 h, while the pure drug solution showed 99.58% of drug released after 2 h only.

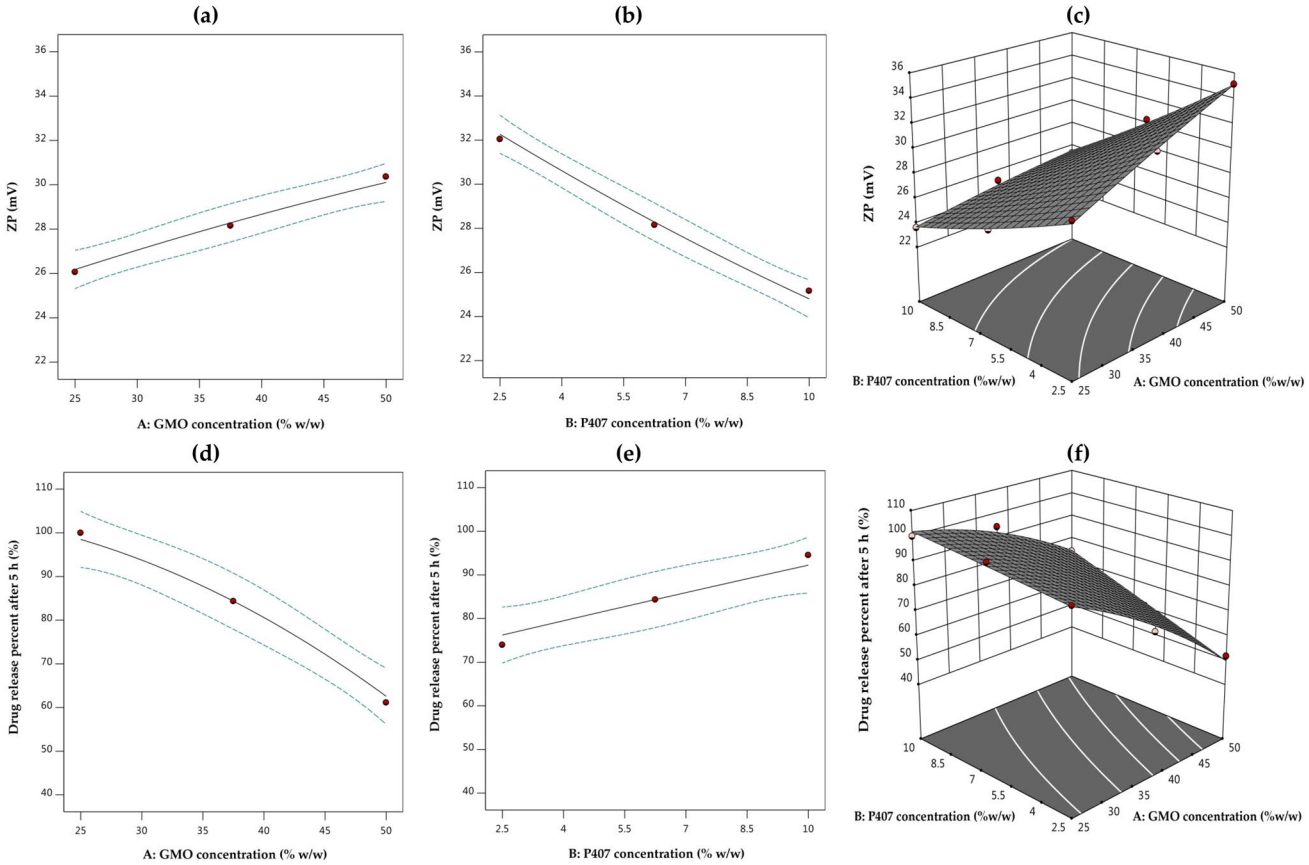

Fig. 2 One factor and 3D response surface graph showing the effect of **a** A on Y_3 **b** B on Y_3 **c** AB on Y_3 **d** A on Y_4 **e** B on Y_4 **f** AB on Y_4

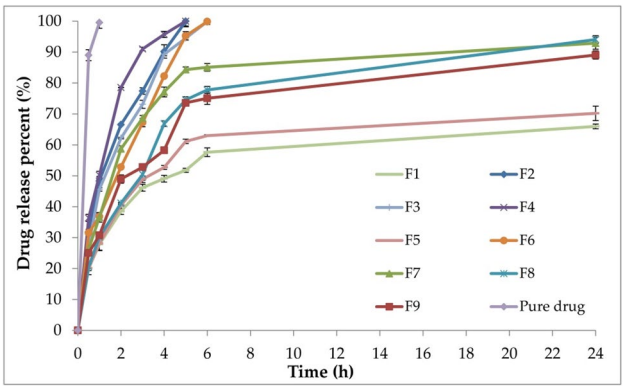

Fig. 3 *In-vitro* release of VRP from different cubosomal formulations (F1-F9) in comparison to pure VRP solution

Characterization of Optimized VRP Cubo-Gel

TEM Imaging

The optimized formulation showed cubic shape to a major extent with no aggregation (Fig. 4b). The presence of P407 could transform the spherical shape of nano-colloidal vesicles to a cubic shape [42]. By TEM study, the optimized formulation exhibited particle size lower than the DLS method. The water molecules around the vesicles might increase the particle size values while following the DLS method in contrast to the TEM method performed at dried state [41]. Suitable particles size lower than 300 nm were reported to favor the passage of drugs through the BBB and achieve the brain targeting [35].

Drug Release Kinetics

The VRP release from the optimized formulation followed the Korsmeyer-Peppas mechanism as indicated from its highest R^2 (0.9286). The n value of Korsmeyer-Peppas model could explain one of the following mechanisms; Fickian (diffusion-controlled) release mechanism ($n \leq 0.43$), non-Fickian (anomalous) release mechanism ($n = 0.43–0.85$), or case II transport (relaxation-controlled) release mechanism ($n \geq 0.85$) [41]. Our results showed that the n value was < 0.43, hence the optimized formulation followed the Fickian release mechanism.

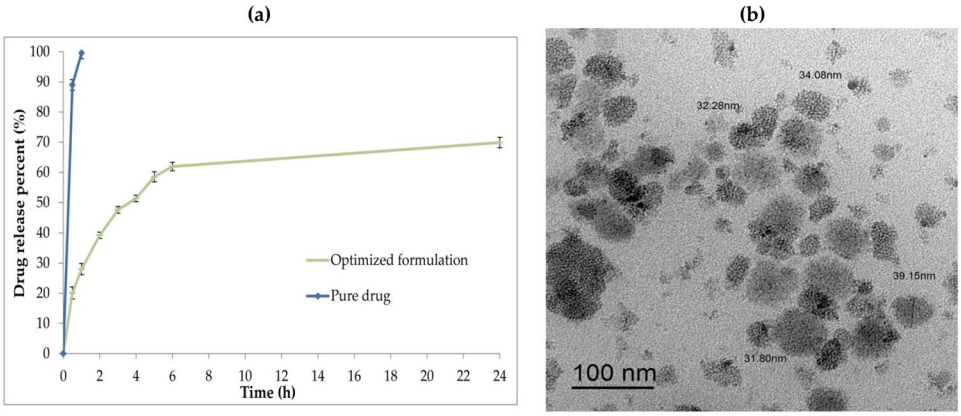

Fig. 4 Characterization of optimized formulation **a** *in-vitro* release in comparison to pure VRP solution **b** TEM micrograph

Stability Study

The optimized formulation demonstrated no alteration in the visual appearance and no significant changes in the four responses tested ($p > 0.05$). This could confirm the acceptable homogeneity and stability of optimized formulation after storage for long time periods.

DSC Study

As shown in Fig. 5, the DSC thermogram of crystalline VRP demonstrated an endothermic peak at 146.35°C corresponding to its melting point [1]. The thermal profiles of GMO and P407 displayed endothermic peaks at 47.03°C and 56.19°C. In the case of blank cubosome, GMO and P407 peaks did not appear. In addition, the thermal behavior of optimized formulation showed absence of the characteristic VRP peak.

Physical Evaluation

The pH of optimized formulation was 6.44 ± 0.2. Besides, the gel strength value was measured as 31.46 ± 0.7 s and the mucoadhesive strength was calculated as 4217.72 ± 68.9 dyne/cm^2. These results would be acceptable for I.N administration.

Ex-vivo Permeation Study

The optimized formulation showed a significantly higher J_{ss} (48.22 ± 2.5 µg.cm^{-2}.h^{-1}) and K_p (0.00964 ± 0.002 cm^{-2}.h^{-1}) values than those of VRP solution (21.37 ± 1.8 µg.cm^{-2}.h^{-1}and 0.00427 ± 0.001 cm^{-2}.h^{-1}, respectively) ($p < 0.05$). In addition, a significant increase in the VRP permeation rate from the optimized formulation was monitored (Fig. 6). It showed a high E_r value (2.26) indicating the enhancement in the permeation of VRP amount per unit area through the sheep nasal membrane from the optimized cubosomes when compared to the drug solution. Ensuring tissue viability throughout experiments is crucial in all cases, and it was evaluated by conducting histological assessment to assess their structural integrity and cellular morphology at the end of permeability experiment [43].

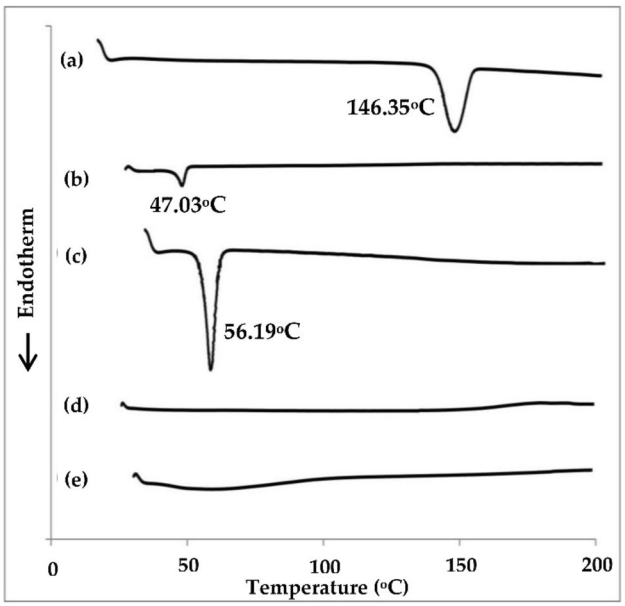

Fig. 5 DSC study of **a** pure VRP powder **b** GMO **c** P407 **d** plain formulation **e** VRP-loaded optimized formulation

Histopathological Evaluation

The epithelial layers of the negative control sample and the sample immersed in PBS overnight for equilibration displayed their entire morphology without damage or inflammation (Fig. 7a, b). The positive control piece exhibited various destructions in the epithelium (Fig. 7c) owing to the action of isopropyl alcohol as a strong mucociliary toxin [11]. In contrast, the epithelial layers of that treated with optimized formulation were kept intact with well-maintained structure and no indications of toxicity (Fig. 7d). These findings could signalize the nasal biocompatibility and safety of

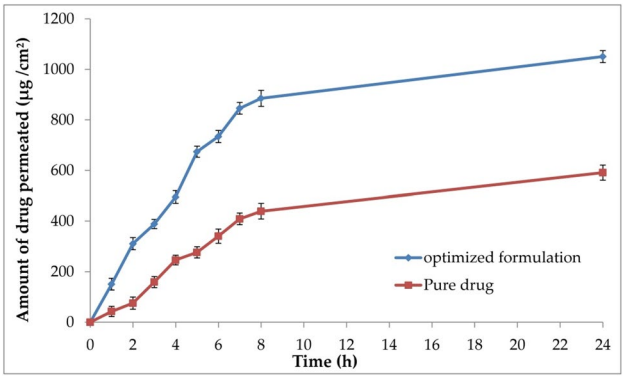

Fig. 6 Ex-vivo permeation study of optimized formulation in comparison to pure VRP solution

the utilized components used in the cubosomes preparation [20, 44, 45].

In-vivo Biodistribution Study

The pharmacokinetic parameters of VRP were studied in the brain and plasma of rats (Table III and Fig. S1 supplementary material) after the I.N administration of both optimized formulation and VRP solution, and the I.V administration of VRP solution. The highest peak of VRP level in the plasma was reached after 30 min consequent to the administration of the I.N optimized formulation and the I.N VRP solution. VRP was expected to be found in the plasma after the I.N administration because the I.N administration could lead to systemic drug absorption. The short T_{max} might be attributed to the fast absorption of VRP through the I.N route [46]. On the other hand, the T_{max} of the drug solution was 10 min after its I.V administration and then declined rapidly. The drug reached its peak in the brain after 30, 60, and 60 min upon administration of I.V VRP solution, I.N optimized formulation, and I.N VRP solution, respectively. The plasma C_{max} values of the I.N optimized formulation and the I.N VRP solution were 560.80 ± 23.9 ng/mL and 410.52 ± 15.2 ng/mL, respectively. Whilst, in the brain tissue, the C_{max} values of the I.N optimized formulation and the I.N VRP solution were 600.82 ± 10.9 ng/mL and 460.51 ± 27.5 ng/mL, respectively. The C_{max} was greater in the brain and plasma for the optimized formulation (I.N) in comparison to the VRP drug solution (I.N).

The $AUC_{0-\infty}$ of the I.N optimized formulation showed the highest value ($128{,}151.39 \pm 137.5$ ng/mL.min) in comparison to the I.N and I.V VRP solutions. This could prove that there was a significant enhancement in the bioavailability of the drug loaded in the optimized formulation in accordance with the sustained release and the good mucoadhesive strength of the optimized formulation [47]. Moreover, the optimized formulation revealed much better bioavailability in the brain than the drug solution (I.V) and this might be

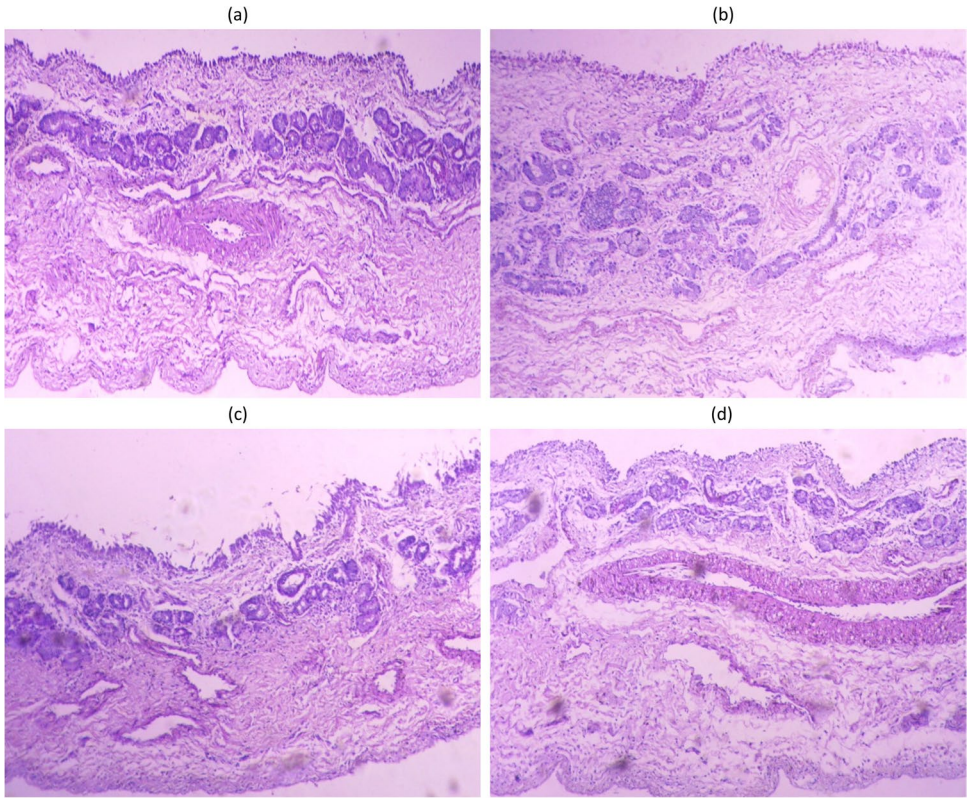

Fig. 7 Histopathological evaluation of nasal sheep mucosal membranes **a** treated with saline **b** immersed in PBS (pH 7.4) containing 0.02% sodium azide overnight for equilibration **c** treated with isopropyl alcohol **d** treated with optimized formulation

Table III *In-vivo* Biodistribtion Study of VRP in Plasma and Brain

Parameter	Plasma			Brain homogenate		
	Optimized cubo-gel (I.N)	Drug solution (I.N)	Drug solution (I.V)	Optimized cubo-gel (I.N)	Drug solution (I.N)	Drug solution (I.V)
C_{max} (ng/mL)	560.80 ± 23.9	410.52 ± 15.2	793.56 ± 20.8	600.82 ± 10.9	460.51 ± 27.5	370.58 ± 15.9
$t_{1/2}$ (min)	183.48 ± 2.2	148.43 ± 6.2	201.68 ± 5.1	315.39 ± 9.2	200.32 ± 7.2	131.44 ± 2.1
T_{max} (min)	30	30	10	60	60	30
$AUC_{0\text{-}24\ h}$ (ng/mL.min)	107,480.55 ± 220.6	68,118.25 ± 135.3	100,531.32 ± 98.6	201,961.85 ± 180.5	101,995.58 ± 150.1	77,468.00 ± 92.4
$AUC_{0\text{-}\infty}$ (ng/mL.min)	128,151.39 ± 137.5	75,658.28 ± 66.2	119,908.40 ± 180.5	333,132.00 ± 162.7	126,690.95 ± 132.6	84,936.58 ± 106.2
BTE% (%)	-	-	-	183.53	41.80	-
DTP% (%)	-	-	-	90.19	59.00	-

I.N, intranasal; I.V, intravenous; C_{max}, maximum plasma concentration; $t_{1/2}$, half-life; T_{max}, time required to reach the C_{max}; $AUC_{0\text{-}24\ h}$, area under the curve; $AUC_{0\text{-}\infty}$, area under the curve from time zero to infinity; BTE%, brain targeting efficiency; DTP%, drug transport percentage

related to bypassing the BBB with direct olfactory transport to the brain.

The I.N optimized formulation had greater BTE% at 183.53% when compared to I.N VRP solution (41.80%). This could suggest the improved brain targeting for the I.N optimized formulation. Additionally, the DTP% of the I.N optimized formulation was 90.19%, but that of the I.N VRP solution was 59.00%. The higher DTP% indicated that the direct olfactory pathway was responsible for the high absorption of VRP in the brain and considered an exclusive access gate to the brain [16, 48].

Discussion

The cubosomal formulations were successfully prepared using the melt dispersion emulsification method. The impacts of changing the concentrations of GMO and P407 on the dependent responses were significantly observed. For illustration, the significant increase in the EE% of cubosmes by increasing GMO concentration could be owing to the nature of the GMO as an amphiphilic polar lipid which could be self-assembled into the bicontinuous cubic structures in water [19]. Raising the GMO amounts could result in increased concentrations of mono-, di-, and triglycerides possessing more space to accommodate excessive drug amounts [49]. Also, this effect might be observed due to the increased viscosity of the medium because increasing the lipid amount resulted in faster solidification of the cubosomal nanoparticles which would prevent the drug diffusion to the external phase of the medium [50]. In contrast, the low encapsulation power of cubosmes as a result of increasing P407 concentration might be due to the escape of VRP into the outer aqueous media. This would be because of the hydrophilic nature of the cubic structure with increasing the P407 levels [51].

The increase in GMO level led to increasing the viscosity of the cubosomal dispersions and thereby their particle size values [16]. On the other hand, the reduction in the particles size with increasing the P407 levels could be related to lowering the interfacial tension between the two immiscible lipid and aqueous phases induced by P407 [52]. Also, P407 as a polymeric surfactant not only could produce a steric stabilization to the system, but also could greatly affect the cubosomal crystalline structure distribution by the stabilizing activity of P407 [53]. Moreover, the range of PDI values less than 0.5 shown by the cubosomal preparations could express their possession of homogeneous distribution and considerable stability. However, nanoparticles of PDI greater than 0.5 could exhibit irregularities in their pharmacokinetic performance and subsequent therapeutic outcomes [41].

Concerning the measurement of ZP of cubosomal formulations, the high surface charge values may aid in the protection of the nanoparticles from aggregating due to the repulsion forces exhibited between the surfaces [54]. Our results indicated that the formulations would have acceptable stability. The marked increase in the ZP of cubosomes by increment of GMO concentration might be due to the ionization of free oleic acid obtained from the GMO, consequently increasing the negative charge on the cubosomes [16]. Whereas, the low ZP values caused by using high concentrations of P407 might be as a result of the non-ionic nature of P407 [29].

By altering the concentrations of GMO and P407, the drug could represent more sustained cumulative release by increasing the concentration of the former component. In contrast, a faster release profile by increasing the concentration of the latter component was exhibited. These results could be attributed to the GMO role as a viscosity enhancer

in delaying the drug partitioning from the oily medium to the aqueous medium, hence decreasing the VRP release [45]. Moreover, the direct relation between increasing the lipid concentration and the increased EE% and PS of the prepared cubosomes could negatively impact on the drug release by decreasing the surface area available for release and lengthening the way through which the drug could diffuse [52]. On the contrary, the rapid release of VRP occurred by the influence of increasing the P407 concentration could be ascribed to the capability of such surfactant for facilitating the solubilization and partitioning of VRP into the external release medium [55]. In addition, P407 could participate in formation of small sized nanoparticles possessing large surface area for drug release [52].

The fast release of drug solution after only 2 h could be due to the high aqueous solubility of the drug and its rapid dissolution in the release medium [37]. On the other hand, the slight initial drug release from the optimized formulation could be explained on the basis of the fast dissolution of the adsorbed drug found at or just below the cubosomal surface. Subsequently, the followed VRP slow release after 24 h might be attributed to the presence of GMO, the most common component of the cubosomes, which delayed the partitioning of VRP from the oily medium to the aqueous medium in addition to the limited diffusion of VRP molecules incorporated in the aqueous channels [20]. In accordance with El Taweel *et al.* [56], the VRP release profile should be beneficial where the initial release of VRP could provide quick relief from pain, while the slower cumulative release shall maintain the patient under prophylaxis over 24 h. In case of stability study, the enhanced stability of optimized formulation could be owing to the amphiphilic nature of P407 [29].

Regarding the DSC study, GMO and P407 peaks disappeared in the thermographs of blank and drug-loaded optimized formulation because both components melted together at close temperatures. This might be due to the plasticizing action of GMO within the polymeric chains which resulted from the bicontinuous structures formed between GMO and aqueous phase in the presence of P407 [57, 58]. In addition, the optimized formulation showed absence of the characteristic VRP peak clarifying its transformation from the crystalline state to the amorphous state and confirming its incorporation inside the formed bicontinuous cubosomal structure between GMO and water [59].

Measuring the pH of an I.N product is mandatory to overcome the irritation of the nasal mucosal. The pH value of optimized cubo-gel was acceptable for the I.N administration with no possible irritancy [60]. Besides, the gel strength value was in the range of 25–50 s which was optimal for the I.N application. Values less than 25 s could indicate the weak gel consistency and the easy gel leakage from the application site. However, values higher than 50 s could indicate the gel hardness and rigidity [32]. Furthermore, the mucoadhesive strength of optimized formulation was ranged between 4,000–6,000 dyne/cm^2 and this could be desirable for nasal gels and help provide a suitable contact time for the gel with the nasal mucosa, hence enhancing the drug absorption afterwards [61].

In comparison to pure VRP solution, the optimized formulation demonstrated an improved VRP permeation through the nasal mucosa. This could be attributed to the nano size of the cubosomal nanoparticles which could penetrate easily into the aqueous pores found in the mucin network [62]. Also, the PS of cubosomes has a significant impact on the cellular uptake and the internalization of the prepared cubosomes. Another explanation might be related to the composition of the optimized formulation. The polar lipid (GMO) could improve the permeation of cubosomes by promoting a structural disorder in the intercellular lipid through an interaction between its hydroxyl group and the anionic oxygen in the phospholipids membrane [29]. In addition, P407 could enhance the permeation ability, therefore improving the mucosal penetration [63].

The improved bioavailability with enhanced brain targeting of the I.N VRP-loaded optimized formulation compared to the I.N drug solution might be attributed to the gel-based formulation which displayed satisfactory sustained VRP release, and reasonable mucoadhesive strength value as shown by the *in-vitro* studies. This was helpful to overcome the challenge of rapid mucociliary clearance when concerning the I.N route [64]. Furthermore, the lipophilic nature of cubosomes could allow efficient penetration with more drug absorption through the mucosal membrane and the BBB. Besides, P407 would participate in enhancing the VRP absorption through its permeation enhancing activity [35]. Higher DTP % and BTE % values indicated that the VRP-loaded optimized formulation could induce a superior brain targeting of the drug.

Conclusion

The present study examined the efficacy of cubosomes to encapsulate hydrophilic VRP of low oral bioavailability as a promising strategy for I.N delivery of VRP for management of episodes of cluster headache. The independent factors of the study were namely, GMO concentration (25–50% w/w) and P407 concentration (2.5–10% w/w). As per the study data, VRP showed more sustained cumulative release by increasing the GMO concentration, however an opposite trend was exhibited by increasing the P407 concentration. There was a direct relation between increasing the GMO concentration and the increased EE%, PS, ZP values of cubosomes. On the other hand, P407 demonstrated its action on decreasing the EE%, PS, and ZP values of cubosomes.

The suggested optimized formulation consisted of GMO (50% w/w) and P407 (5.5% w/w). The optimized cubo-gel formulation showed acceptable physical properties in terms of pH, gel strength, and mucoadhesive strength in addition to nasal permeation properties. The I.N optimized formulation exhibited significant enhancement of bioavailability and higher DTP% and BTE% in comparison to the I.N and I.V VRP solution which confirmed the high nasal mucoadhesion with bypassing the first pass effect. Consequently, the optimal cubosomal formulation may be an outstanding biocompatible dosage form for brain targeting of VRP via the I.N route.

Supplementary Information The online version contains supplementary material available at https://doi.org/10.1208/s12249-024-02814-w.

Authors' Contributions Mennatullah M. Faisal: Conceptualization, Methodology, Software, Formal analysis, Writing—original draft preparation. Writing—review and editing. Eman Gomaa: Conceptualization, Methodology, Formal analysis, Data curation, Writing—original draft preparation, Writing—review and editing. Adel Ehab Ibrahim: Methodology, Analysis, Writing—review and editing. Sami El Deeb: Methodology, Funding acquisition. Ahmed Al-Harrasi: Data curation, Funding acquisition. Tarek M. Ibrahim: Methodology, Software, Data curation, Writing—original draft preparation, Writing—review and editing.

Funding Open Access funding enabled and organized by Projekt DEAL. This research has no funding to declare.

Data Availability All data are available from the corresponding author upon reasonable request.

Declarations

Ethics Approval and Consent to Participate The animal experiments were performed according to the guidelines of Institutional Animal Care and Use Committee (IACUC) of Faculty of Pharmacy, Zagazig University, Egypt (ZU-IACUC/3/F/49/2022).

Consent for Publication Not applicable.

Competing Interests The authors declare that they have no competing interests.

References

1. Qian H, Chen D, Xu X, Li R, Yan G, Fan T. FDM 3D-printed sustained-release gastric-floating verapamil hydrochloride formulations with cylinder, capsule and hemisphere shapes, and low infill percentage. Pharmaceutics. 2022;14(2):281.
2. Petersen AS, Barloese MC, Snoer A, Soerensen AMS, Jensen RH. Verapamil and cluster headache: still a mystery. A narrative review of efficacy, mechanisms and perspectives. Headache. 2019;59(8):1198–211.
3. Diener HC, May A. Drug Treatment of Cluster Headache. Drugs. 2022;82(1):33–42. https://doi.org/10.1007/s40265-021-01658-z.
4. Leone M, D'amico D, Frediani F, Moschiano F, Grazzi L, Attanasio A, et al. Verapamil in the prophylaxis of episodic cluster headache: a double-blind study versus placebo. Neurology. 2000;54(6):1382–5.
5. Rusanen SS, De S, Schindler EAD, Artto VA, Storvik M. Self-Reported Efficacy of Treatments in Cluster Headache: a Systematic Review of Survey Studies. Curr Pain Headache Rep. 2022;26(8):623–37.
6. Fahie S, Cassagnol M. Verapamil. StatPearls [Internet]: StatPearls Publishing; 2023.
7. Brandt R, Haan J, Terwindt G, Fronczek R. Cluster headache and pain: Features and treatments. Features and Assessments of Pain, Anaesthesia, and Analgesia: Elsevier; 2022. p. 93–104.
8. CALAN® SR (verapamil hydrochloride)Sustained-Release Oral Caplets United States FDA. 2023. Accessed September 2023.
9. Mouez MA, Zaki NM, Mansour S, Geneidi AS. Bioavailability enhancement of verapamil HCl via intranasal chitosan microspheres. Eur J Pharm Sci. 2014;51:59–66.
10. Francis GJ, Becker WJ, Pringsheim TM. Acute and preventive pharmacologic treatment of cluster headache. Neurology. 2010;75(5):463–73.
11. Abdulla NA, Balata GF, El-Ghamry HA, Gomaa E. Intranasal delivery of Clozapine using nanoemulsion-based in-situ gels: An approach for bioavailability enhancement. Saudi Pharm J. 2021;29(12):1466–85.
12. Anselmo AC, Gokarn Y, Mitragotri S. Non-invasive delivery strategies for biologics. Nat Rev Drug Discovery. 2019;18(1):19–40.
13. Narayan R, Singh M, Ranjan O, Nayak Y, Garg S, Shavi GV, et al. Development of risperidone liposomes for brain targeting through intranasal route. Life Sci. 2016;163:38–45.
14. Sita V, Jadhav D, Vavia P. Niosomes for nose-to-brain delivery of bromocriptine: Formulation development, efficacy evaluation and toxicity profiling. J Drug Deliv Sci Technol. 2020;58: 101791.
15. Abo El-Enin HA, Elkomy MH, Naguib IA, Ahmed MF, Alsaidan OA, Alsalahat I, et al. Lipid nanocarriers overlaid with chitosan for brain delivery of berberine via the nasal route. Pharmaceuticals. 2022;15(3):281.
16. Eissa EM, Elkomy MH, Eid HM, Ali AA, Abourehab MA, Alsubaiyel AM, et al. Intranasal delivery of granisetron to the brain via nanostructured cubosomes-based in situ gel for improved management of chemotherapy-induced emesis. Pharmaceutics. 2022;14(7):1374.
17. Sonvico F, Clementino A, Buttini F, Colombo G, Pescina S, StanisçuaskiGuterres S, et al. Surface-modified nanocarriers for nose-to-brain delivery: from bioadhesion to targeting. Pharmaceutics. 2018;10(1):34.
18. Abourehab MA, Ansari MJ, Singh A, Hassan A, Abdelgawad MA, Shrivastav P, et al. Cubosomes as an emerging platform for drug delivery: A review of the state of the art. J Mater Chem B. 2022;10(15):2781–819.
19. Gaballa SA, El Garhy OH, Abdelkader H. Cubosomes: composition, preparation, and drug delivery applications. J Adv Biomed Pharm Sci. 2020;3(1):1–9.

20. Nasr M, Ghorab MK, Abdelazem A. In vitro and in vivo evaluation of cubosomes containing 5-fluorouracil for liver targeting. Acta Pharm Sin B. 2015;5(1):79–88.
21. Umar H, Wahab HA, Gazzali AM, Tahir H, Ahmad W. Cubosomes: Design, Development, and Tumor-Targeted Drug Delivery Applications. Polymers. 2022;14(15):3118.
22. Badie H, Abbas H. Novel small self-assembled resveratrol-bearing cubosomes and hexosomes: Preparation, charachterization, and ex vivo permeation. Drug Dev Ind Pharm. 2018;44(12):2013–25.
23. Benkő E, Ilič IG, Kristó K, Regdon G Jr, Csóka I, Pintye-Hódi K, et al. Predicting drug release rate of implantable matrices and better understanding of the underlying mechanisms through experimental design and artificial neural network-based modelling. Pharmaceutics. 2022;14(2):228.
24. Hafez HM, El Deeb S, Mahmoud Swaif M, Ismail Ibrahim R, Ali Kamil R, Salman Abdelwahed A, et al. Micellar Organic-solvent Free HPLC Design of Experiment for the Determination of Ertapenem and Meropenem; Assessment using GAPI, AGREE and Analytical Eco-scale models. Microchem J. 2023;185: 108262. https://doi.org/10.1016/j.microc.2022.108262.
25. Alara O, Abdurahman N, Olalere O. Ethanolic extraction of flavonoids, phenolics and antioxidants from Vernonia amygdalina leaf using two-level factorial design. J King Saud Univ-Sci. 2020;32(1):7–16.
26. Lombardo M, Espósito BP, Lourenço FR, Kaneko TM. The application of pharmaceutical quality by design concepts to evaluate the antioxidant and antimicrobial properties of a preservative system including desferrioxamine. DARU J Pharm Sci. 2020;28:635–46.
27. Elkomy MH, Alruwaili NK, Elmowafy M, Shalaby K, Zafar A, Ahmad N, et al. Surface-modified bilosomes nanogel bearing a natural plant alkaloid for safe management of rheumatoid arthritis inflammation. Pharmaceutics. 2022;14(3):563.
28. Elkomy MH, El Menshawe SF, Eid HM, Ali AM. Development of a nanogel formulation for transdermal delivery of tenoxicam: a pharmacokinetic–pharmacodynamic modeling approach for quantitative prediction of skin absorption. Drug Dev Ind Pharm. 2017;43(4):531–44.
29. Elsenosy FM, Abdelbary GA, Elshafeey AH, Elsayed I, Fares AR. Brain targeting of duloxetine HCL via intranasal delivery of loaded cubosomal gel: in vitro characterization, ex vivo permeation, and in vivo biodistribution studies. Int J Nanomedicine. 2020:9517–37.
30. Ibrahim TM, Abdallah MH, El-Megrab NA, El-Nahas HM. Transdermal ethosomal gel nanocarriers; a promising strategy for enhancement of anti-hypertensive effect of carvedilol. J Liposome Res. 2019;29(3):215–28.
31. Shoman NA, Gebreel RM, El-Nabarawi MA, Attia A. Optimization of hyaluronan-enriched cubosomes for bromfenac delivery enhancing corneal permeation: characterization, ex vivo, and in vivo evaluation. Drug Delivery. 2023;30(1):2162162.
32. Ibrahim TM. Exploitation of transdermal nanobilosomal gel platforms for ameliorating anti-diabetic activity of empagliflozin following I-optimal design. J Drug Deliv Sci Technol. 2023;84: 104455.
33. Balata GF, Faisal MM, Elghamry HA, Sabry SA. Preparation and characterization of ivabradine HCl transfersomes for enhanced transdermal delivery. J Drug Deliv Sci Technol. 2020;60: 101921.
34. Lee YS, Yoon JN, Yoon I-S, Lee MG, Kang HE. Pharmacokinetics of verapamil and its metabolite norverapamil in rats with hyperlipidaemia induced by poloxamer 407. Xenobiotica. 2012;42(8):766–74.
35. Ahirrao M, Shrotriya S. In vitro and in vivo evaluation of cubosomal in situ nasal gel containing resveratrol for brain targeting. Drug Dev Ind Pharm. 2017;43(10):1686–93.
36. Eid HM, Elkomy MH, El Menshawe SF, Salem HF. Transfersomal nanovesicles for nose-to-brain delivery of ofloxacin for better management of bacterial meningitis: Formulation, optimization by Box-Behnken design, characterization and in vivo pharmacokinetic study. J Drug Deliv Sci Technol. 2019;54: 101304.
37. Mouez MA, Nasr M, Abdel-Mottaleb M, Geneidi AS, Mansour S. Composite chitosan-transfersomal vesicles for improved transnasal permeation and bioavailability of verapamil. Int J Biol Macromol. 2016;93:591–9.
38. Mehanna MM, Abla KK, Domiati S, Elmaradny H. Superiority of microemulsion-based hydrogel for non-steroidal anti-inflammatory drug transdermal delivery: a comparative safety and antinociceptive efficacy study. Int J Pharm. 2022;622: 121830.
39. Ibrahim TM, Ayoub MM, El-Bassossy HM, El-Nahas HM, Gomaa E. Investigation of Alogliptin-Loaded In Situ Gel Implants by 23 Factorial Design with Glycemic Assessment in Rats. Pharmaceutics. 2022;14(9):1867.
40. Hosny KM, Rizg WY, Khallaf RA. Preparation and optimization of in situ gel loaded with rosuvastatin-ellagic acid nanotransfersomes to enhance the anti-proliferative activity. Pharmaceutics. 2020;12(3):263.
41. Attia MS, Radwan MF, Ibrahim TS, Ibrahim TM. Development of Carvedilol-Loaded Albumin-Based Nanoparticles with Factorial Design to Optimize In Vitro and In Vivo Performance. Pharmaceutics. 2023;15(5):1425.
42. El-Shenawy AA, Elsayed MM, Atwa GM, Abourehab MA, Mohamed MS, Ghoneim MM, et al. Anti-Tumor Activity of Orally Administered Gefitinib-Loaded Nanosized Cubosomes against Colon Cancer. Pharmaceutics. 2023;15(2):680.
43. Machado A, Neves Jd. 4.5 - Tissue-based in vitro and ex vivo models for vaginal permeability studies. In: Sarmento B, editor. Concepts and Models for Drug Permeability Studies: Woodhead Publishing; 2016. p. 273–308.
44. Kaul S, Nagaich U, Verma N. Preclinical assessment of nanostructured liquid crystalline particles for the management of bacterial keratitis: in vivo and pharmacokinetics study. Drug Delivery and Translational Research. 2022:1–19.
45. Abdelrahman FE, Elsayed I, Gad MK, Badr A, Mohamed MI. Investigating the cubosomal ability for transnasal brain targeting: in vitro optimization, ex vivo permeation and in vivo biodistribution. Int J Pharm. 2015;490(1–2):281–91.
46. Alharbi WS, Hareeri RH, Bazuhair M, Alfaleh MA, Alhakamy NA, Fahmy UA, et al. Spanlastics as a potential platform for enhancing the brain delivery of flibanserin: in vitro response-surface optimization and in vivo pharmacokinetics assessment. Pharmaceutics. 2022;14(12):2627.
47. Bhatt M, Bhatt GK. An overview: Formulation and product development of nasal spray. World J Pharm Res. 2017;6:404–13.
48. Natarajan J, Baskaran M, Humtsoe LC, Vadivelan R, Justin A. Enhanced brain targeting efficacy of Olanzapine through solid lipid nanoparticles. Artif Cells Nanomed Biotechnol. 2017;45(2):364–71.
49. Thakkar V, Korat V, Baldaniya L, Gohel M, Gandhi T, Patel N. Development and characterization of novel hydrogel containing antimicrobial drug for treatment of burns. Int J Pharm Investig. 2016;6(3):158.
50. El-Enin HA, Al-Shanbari AH. Nanostructured liquid crystalline formulation as a remarkable new drug delivery system of anti-epileptic drugs for treating children patients. Saudi Pharm J. 2018;26(6):790–800.
51. Patil RP, Pawara DD, Gudewar CS, Tekade AR. Nanostructured cubosomes in an in situ nasal gel system: an alternative approach for the controlled delivery of donepezil HCl to brain. J Liposome Res. 2019;29(3):264–73.
52. Said M, Aboelwafa AA, Elshafeey AH, Elsayed I. Central composite optimization of ocular mucoadhesive cubosomes for

enhanced bioavailability and controlled delivery of voriconazole. J Drug Deliv Sci Technol. 2021;61: 102075.
53. Pitto-Barry A, Barry NP. Pluronic® block-copolymers in medicine: from chemical and biological versatility to rationalisation and clinical advances. Polym Chem. 2014;5(10):3291–7.
54. Eid HM, Naguib IA, Alsantali RI, Alsalahat I, Hegazy AM. Novel chitosan-coated niosomal formulation for improved management of bacterial conjunctivitis: a highly permeable and efficient ocular nanocarrier for azithromycin. J Pharm Sci. 2021;110(8):3027–36.
55. Nasr M, Dawoud M. Sorbitol based powder precursor of cubosomes as an oral delivery system for improved bioavailability of poorly water soluble drugs. J Drug Deliv Sci Technol. 2016;35:106–13.
56. El Taweel MM, Aboul-Einien MH, Kassem MA, Elkasabgy NA. Intranasal Zolmitriptan-Loaded Bilosomes with Extended Nasal Mucociliary Transit Time for Direct Nose to Brain Delivery. Pharmaceutics. 2021;13(11):1828.
57. Bei D, Zhang T, Murowchick JB, Youan B-BC. Formulation of dacarbazine-loaded cubosomes. Part III. Physicochemical characterization. AAPS PharmSciTech. 2010;11:1243–9.
58. Younes NF, Abdel-Halim SA, Elassasy AI. Corneal targeted Sertaconazole nitrate loaded cubosomes: preparation, statistical optimization, in vitro characterization, ex vivo permeation and in vivo studies. Int J Pharm. 2018;553(1–2):386–97.
59. Mohsen AM, Younis MM, Salama A, Darwish AB. Cubosomes as a potential oral drug delivery system for enhancing the hepatoprotective effect of coenzyme Q10. J Pharm Sci. 2021;110(7):2677–86.
60. Gu F, Fan H, Cong Z, Li S, Wang Y, Wu C. Preparation, characterization, and in vivo pharmacokinetics of thermosensitive s nasal gel of donepezil hydrochloride. Acta Pharm. 2020;70(3):411–22.
61. Wang Y, Jiang S, Wang H, Bie H. A mucoadhesive, thermoreversible in situ nasal gel of geniposide for neurodegenerative diseases. PLoS ONE. 2017;12(12): e0189478.
62. Jampílek J, Kralova K. Natural biopolymeric nanoformulations for brain drug delivery. Nanocarriers for Brain Targetting: Principles and Applications; Keservani, RK, Sharma, AK, Kesharwani, RK, Eds. 2019:131–203.
63. Agiba AM, Nasr M, Abdel-Hamid S, Eldin AB, Geneidi AS. Enhancing the intestinal permeation of the chondroprotective nutraceuticals glucosamine sulphate and chondroitin sulphate using conventional and modified liposomes. Curr Drug Deliv. 2018;15(6):907–16.
64. Mahajan HS, Mahajan MS, Nerkar PP, Agrawal A. Nanoemulsion-based intranasal drug delivery system of saquinavir mesylate for brain targeting. Drug Delivery. 2014;21(2):148–54.